

Scale-invariant multilevel Monte Carlo method and application to linear elasticity

Sharana Kumar Shivanand^{a*}, Bojana Rosić^b

^aInstitute of Scientific Computing, Technische Universität Braunschweig, Germany

^bApplied Mechanics and Data Analysis, University of Twente, Netherlands

July 28, 2023

Abstract

We propose a novel scale-invariant version of the mean and variance multi-level Monte Carlo estimate. The computation cost across grid levels is optimised using a normalized error based on t-statistics. By doing so, the algorithm achieves convergence independent of the physical scale at which the estimate is computed. The effectiveness of this algorithm is demonstrated through testing on a linear elastic example, where material uncertainty incorporating both heterogeneity and anisotropy is considered in the constitutive law.

Keywords: Monte Carlo, multilevel Monte Carlo, normalized error, uncertainty quantification, linear elasticity

1 Introduction

In forward problems, estimation of statistics to characterize a stochastic solution of a stochastic partial differential equation or an ordinary differential equation is of utmost importance in uncertainty quantification (UQ). In this regard, one of the fundamental objectives of UQ is to determine second-order statistical moments, notably the mean and variance. Unlike skewness and kurtosis (the third and fourth moments, respectively), which are dimensionless, the mean and variance are scale-dependent measures, which are commonly determined using absolute error estimates such as the mean square error (MSE) or the root mean square error (RMSE). This further means that the statistical convergence of the algorithm is dependent on the scale or magnitude of the quantity of interest (QoI). Hence, a performance comparison between different estimators (here, mean and variance) or individual estimators on different scales cannot be done. To overcome this, normalized error estimates play a crucial role in statistics by providing a standardised measure of the accuracy or precision of statistical estimates or predictions.

In the last few decades, numerous algorithms—to name a few such as surrogates, direct integration, and variance reduction methods—have been developed for performing efficient forward uncertainty propagation [38, 35, 26]. Among these algorithms, the Monte Carlo

*Corresponding author. E-mail: sshivanand@turing.ac.uk

method (MC) has traditionally been regarded as the gold standard for solving stochastic problems, due to its resilience against the curse of dimensionality [27, 12, 16]. However, despite its appeal, the practical implementation of MC often faces challenges due to slow convergence and the substantial computational effort it demands. To address these limitations, recent scientific attention has shifted towards a more computationally efficient approach known as the sampling-based multilevel Monte Carlo method (MLMC). This algorithm has emerged as a promising alternative to MC, offering improved computational adequacy. The key to MLMC's success lies in spreading out the sampling strategy across a hierarchy of different fidelity levels such that the number of stochastic samples drastically decays with the increment in fidelity of the model. Under the right conditions, this results in an overall reduction of the computational cost as compared to MC, making MLMC an attractive option for practical applications.

To the best of the authors' knowledge, the MLMC was first introduced by [20] in the context of estimating multi-dimensional parameter-dependent integrals and is further employed by [14] for solving Itô's stochastic ordinary differential equations in the computational finance application. Following this, the MLMC is extended to solve the linear elliptic PDEs describing the subsurface flow with inhomogeneous stochastic parameters [7, 2], whereas the extension to the random field scenario is studied in [7, 36]. However, previously mentioned works focused only on the approximation of the output response sample mean and therefore lacked full characterization of the probabilistic solution. Consequently, [28] studies the unbiased MLMC sample variance estimator, which is further analysed in [3] on a class of elliptic random obstacle problems. An alternative MLMC variance estimator based on h-statistics [9, 29] is introduced in [25]. Though the estimation of other higher-order moments such as skewness and kurtosis through MLMC is out of the scope of this paper, more literature on this can be found [4, 25].

In the context of assessing the computation efficiency of the MLMC algorithm in a standardised manner, the authors in [3] theoretically prove, with specific assumptions on the deterministic solution, two error bounds for the multilevel sample mean and variance that may be directly compared. But no normalized error estimates are defined for practical interpretation of the complexities between the moments. On the other hand, relative error estimates, where the total MSE of a given moment is normalized by the square of its own statistic, are considered in [25]. However, such ratios are not fully non-dimensional, especially for linear transformations involving an operation of addition by a scalar with the QoI. Therefore, to tackle this issue, in this article, we propose novel scale-invariant or normalized mean square error (NMSE) estimates for the MLMC mean and variance estimations, based on t-statistics [34, 11]. The newly introduced relative errors are statistically defined, with chosen normalizing factors that are finite, unbiased, and of minimal variance. They also ensure the total MSE of the MLMC algorithm is normalized under any linear transformation (scaling and addition) of QoI. Furthermore, we also define standardised errors for the MC mean and variance estimators. Thereby, the dimensionless error estimates can be used for an easier comparison of not only the MLMC mean and variance estimates but also the corresponding MC ones, thus improving the overall interpretability of the MC and MLMC algorithms.

The other objective of this paper is to investigate the applicability of the scale-invariant MLMC method to linear elliptic problems described by stochastic parameters representing both heterogeneity and uncertain material symmetries. As an example, we consider the linear-elastic material model of the human femoral bone, whose constitutive law is assumed to be uncertain. In particular, the bone material symmetry is described as uncer-

tain due to the lack of conclusive verification of the class of elastic symmetry the human femur belongs to [31, 23]. Hence, the entire elasticity tensor is constructed as random with a predefined elastic symmetry in the mean (orthotropy [13] in this case) and purely arbitrary symmetries in each stochastic realization. Consequently, the positive-definite random elasticity matrices are modelled as matrix-valued random fields, as proposed in [32, 33]. In this work, we restrict ourselves to material uncertainties only, assuming that the remaining model parametrization is deterministic. However, the numerical approach is general enough to be employed for other types of uncertainties as well.

The paper is organised as follows: In Section 2, we describe the problem; the theoretical procedure of scale-invariant MC mean and variance estimates are elaborated in Section 3. Following this, in Section 4, the normalized versions of the MLMC mean and variance estimators are detailed. A deterministic and stochastic setting of the linear elastic material model, along with the stochastic material modelling, is given in Section 5. In Section 6, the numerical results of the normalized MLMC and MC when implemented on a two-dimensional proximal femur are explained. Finally, the conclusions are drawn in Section 7.

2 Problem description

Let us consider a physical system occupying the spatial domain $\mathcal{G} \subset \mathbb{R}^d$ in a d -dimensional Euclidean space, modelled by an abstract equilibrium equation:

$$\mathcal{A}(q(x), u(x)) = f(x). \quad (1)$$

Here, $u(x) \in \mathcal{U}$ describes the state of the system at a spatial point $x \in \mathcal{G}$ lying in a Hilbert space \mathcal{U} (for the sake of simplicity), \mathcal{A} is a (possibly non-linear) operator modelling the physics of the system, and $f \in \mathcal{U}^*$ is some external influence (action/excitation/loading). Furthermore, we assume that the model depends on the parameter set $q \in \mathcal{Q}$ and that it is accompanied by appropriate boundary and/or initial conditions. Note that, for brevity, the model in the previous equation describes the physical system only in a spatial domain x , whereas one may also generalise this to time-dependent processes.

The uncertainty in the previous equation may arise due to the randomness in external influence f , initial or boundary conditions, geometry \mathcal{G} , as well as the coefficient of operator \mathcal{A} , i.e., parameter q . Although the theory presented further does not depend on this choice and is general enough to cover all of the mentioned (single or combination of) cases, this article focuses on incorporating stochasticity only in coefficient q . In the theory of continuum solid mechanics, the parameter q represents one of the very well-known physical phenomena, such as elasticity, which is detailed as an example in Section 5. Here, we assume that q is modelled as a random field $q(x, \omega)$ with finite second-order moments on a probability space $(\Omega, \mathfrak{F}, \mathbb{P})$, where Ω denotes the set of elementary events, \mathfrak{F} is a σ -algebra of events, and \mathbb{P} is a probability measure. Following this, Eq. (1) rewrites to a stochastic form:

$$\mathcal{A}(q(x, \omega), u(x, \omega)) = f(x), \quad (2)$$

which further is to be solved for $u(x, \omega) \in \mathcal{U} \otimes L_2(\Omega, \mathfrak{F}, \mathbb{P})$.

Often, when the response of a model is uncertain, one is interested in attaining its relevant information via its corresponding statistics. Analytically, these statistical moments of the solution $u \equiv u(x, \omega)$ can be represented as r -th, $r \in \mathbb{N}$, central moment:

$$\mathbb{E}((u - \mathbb{E}(u))^r) = \int_{\Omega} (u - \mathbb{E}(u))^r \mathbb{P}(d\omega) \quad (3)$$

with $\mu(u) := \mathbb{E}(u)$ being the mean or the first raw moment and $\text{Var}(u) := \mathbb{E}((u - \mathbb{E}(u))^2)$ being the second central moment or the variance. Similarly, the central moments at values $r = 3$ and $r = 4$ represent the skewness and kurtosis, respectively. However, the objective of this study is to determine the first two moments (i.e., mean and variance) only after an appropriate deterministic discretization of the problem in Eq. (2) is presented.

Due to spatial and stochastic dependence, the solution $u \equiv u(x, \omega)$ in Eq. (2) is first discretized in a spatial domain, i.e., we search for the solution in a finite subspace $\mathcal{U}_h \subset \mathcal{U}$. After rewriting the problem in Eq. (2) in a variational form, the spatial discretization $u_h(x, \omega) \in \mathcal{U}_h$ — h being the discretization parameter—can take the finite element form on a sufficiently fine spatial grid \mathcal{T}_h ¹. The expectation functional in Eq. (3) then rewrites to:

$$\mathbb{E}((u_h - \mathbb{E}(u_h))^r) = \int_{\Omega} (u_h - \mathbb{E}(u_h))^r \mathbb{P}(d\omega), \quad (4)$$

in which the exact solution u is substituted by a semi-discretized solution $u_h \equiv u_h(x, \omega)$.

3 Monte Carlo method

Due to the complexity of integrating Eq. (4) analytically, in this paper, the focus is on the sampling-based Monte Carlo (MC) method [27, 12]. The MC estimators further employ multi-level approximation of the finite element solution u_h , also known as the multi-level Monte Carlo (MLMC) method [20, 14, 15], in Section 4.

3.1 Monte Carlo estimation of mean

For an unbiased estimate of the statistic $g(\omega)$, one may take a symmetric function

$$\hat{\mu}^{\text{MC}}(g) = \frac{1}{N}(g(\omega_1) + g(\omega_2) + \dots + g(\omega_N)), \quad (5)$$

meaning that the estimate does not depend on the order in which observations were taken. The existence and uniqueness of such a choice are given in [19]. Under the assumption that each sample $u_h(x, \omega_i)$ comes from the identical distribution as $u_h(x, \omega)$ and by use of Eq. (5), one may reformulate the MC estimate of the mean $\mu(u_h)$ as [27, 12]

$$\hat{\mu}^{\text{MC}}(u_{h,N}) = \frac{1}{N} \sum_{i=1}^N u_h(x, \omega_i), \quad (6)$$

where N is the sample size of the random field $u_h(x, \omega)$ at a spatial location x . Following this, the approximation error of the MC-based mean estimate $\hat{\mu}^{\text{MC}} \equiv \hat{\mu}^{\text{MC}}(u_{h,N})$ compared to the exact mean reads

$$e(\hat{\mu}^{\text{MC}}) = \hat{\mu}^{\text{MC}} - \mathbb{E}(u), \quad (7)$$

which further can be rewritten as

$$e(\hat{\mu}^{\text{MC}}) = \hat{\mu}^{\text{MC}} - \mathbb{E}(u_h) + \mathbb{E}(u_h) - \mathbb{E}(u). \quad (8)$$

Thus, the mean square error (MSE) reads

$$\begin{aligned} \varepsilon(\hat{\mu}^{\text{MC}}) &:= \mathbb{E}(e^2) = \mathbb{E}((\hat{\mu}^{\text{MC}} - \mathbb{E}(u_h) + \mathbb{E}(u_h) - \mathbb{E}(u))^2) \\ &= \mathbb{E}((\hat{\mu}^{\text{MC}} - \mathbb{E}(u_h))^2) + (\mathbb{E}(u_h) - \mathbb{E}(u))^2 + \\ &\quad 2(\mathbb{E}(u_h) - \mathbb{E}(u))(\mathbb{E}(\hat{\mu}^{\text{MC}}) - \mathbb{E}(u_h)), \end{aligned} \quad (9)$$

¹Other types of discretization techniques can be considered as well

in which $\hat{\mu}^{\text{MC}}$ is assumed to be an unbiased estimator; meaning that $\mathbb{E}(\hat{\mu}^{\text{MC}}) = \mathbb{E}(u_h)$, and also, $\mathbb{E}((\hat{\mu}^{\text{MC}} - \mathbb{E}(u_h))^2) = \text{Var}(\hat{\mu}^{\text{MC}}) = \text{Var}(u_h)/N$. Therefore, the previous equation reduces to:

$$\varepsilon(\hat{\mu}^{\text{MC}}) = \frac{\text{Var}(u_h)}{N} + (\mathbb{E}(u_h) - \mathbb{E}(u))^2. \quad (10)$$

The first term in the previous equation is the sampling error $\varepsilon_s(\hat{\mu}^{\text{MC}})$, which varies inversely to the sample size N . On the other hand, the second term describes square of the spatial discretization error i.e. $\varepsilon_d^2(\hat{\mu}^{\text{MC}}) := (\mathbb{E}(u_h) - \mathbb{E}(u))^2$, whose change is proportional to the element size h .

3.1.1 Scale-invariant error estimator for Monte Carlo mean estimation

The MSE in Eq. (10) is an absolute error estimate and, hence, scale-dependent. Meaning that, if each observation $u_h(x, \omega_i)$ is linearly transformed in the form $a u_h(x, \omega_i) + b$, in which $a, b \in \mathbb{R}$ are constants, then the Monte Carlo error in Eq. (10) will be affected in a square proportional manner—as

$$\text{Var}(a u_h + b) = a^2 \text{Var}(u_h) \quad (11)$$

and

$$(\mathbb{E}(a u_h + b) - \mathbb{E}(a u + b))^2 = a^2 (\mathbb{E}(u_h) - \mathbb{E}(u))^2. \quad (12)$$

For instance, consider a scenario of transforming the units of temperature (e.g., in heat transfer) from Kelvin (K) to degree Fahrenheit ($^{\circ}\text{F}$), i.e., $^{\circ}\text{F} = 9/5(\text{K} - 273.15) + 32$ or the units of the displacement field—in mechanics—from a millimetre (mm) to a metre (m), i.e., $\text{m} = 10^{-3}\text{mm}$. Consequently, the absolute error defined in Eq. (10) is now read in newly transformed units ($^{\circ}\text{F}$ or m) instead of the original units (K or mm).

This leads to an issue of non-standardised proficiency comparison of MC complexity between such two differently scaled entities, which is not suitable in practical applications. Moreover, a further complication arises when one wants to compare convergence between two different MC moments for a given magnitude of MSE. As an example, under linear transformation as shown in Eqs. (11) and (12), the MSE in the MC mean estimator is scaled by a factor of a^2 , whereas in the MC variance estimate, the scaling unit a would be set to the power of four; more information on this will follow in Section 3.2. To overcome this issue, one must define a scale-invariant version of MSE as defined in Eq. (10). To this end, we introduce a statistical normalizing function for the MC mean estimate $\zeta_m(u_h)$ that must inhibit the following properties:

- (a) It should satisfy the condition $\zeta_m(a u_h + b) = a^2 \zeta_m(u_h)$.
- (b) It must be finite and greater than zero, i.e., $0 < \zeta_m(u_h) < \infty$.
- (c) It should be unbiased and of minimum variance.

Keeping this in mind, as per t-statistics, we consider $\zeta_m(u_h) = \text{Var}(u_h)$ as a normalization entity [34, 11], given that $0 < \text{Var}(u_h) < \infty$ (meets the second requirement). Clearly, $\text{Var}(u_h)$ satisfies the first condition (see Eq. (11)), unlike the common practise of taking the square of the mean value $\mathbb{E}(u_h)^2$ as a standardising constant, which violates this requirement. Following this, the new type of standardised error estimate is defined as

$$\hat{e}(\hat{\mu}^{\text{MC}}) := \frac{e(\hat{\mu}^{\text{MC}})}{\sqrt{\zeta_m(u_h)}}. \quad (13)$$

Finally, by normalizing Eq. (10), one obtains the squared error estimate

$$\hat{\varepsilon}(\hat{\mu}^{\text{MC}}) := \mathbb{E}(\hat{\varepsilon}^2) = \frac{1}{N} + \frac{(\mathbb{E}(u_h) - \mathbb{E}(u))^2}{\zeta_m(u_h)}, \quad (14)$$

in which the first term is the scale-invariant sampling accuracy $\hat{\varepsilon}_s(\hat{\mu}^{\text{MC}})$, and the second term represents the square of the new normalized discretization error, $\hat{\varepsilon}_d^2(\hat{\mu}^{\text{MC}}) := \varepsilon_d^2/\zeta_m(u_h)$.

3.1.2 Unbiased estimation of MC mean normalizing function

As in general, the variance $\text{Var}(u_h)$ is not known; it is estimated. For this purpose, one may use the estimator $\hat{\text{Var}}^{\text{MC}}(u_{h,N})$, which is determined by the MC procedure with N random draws. However, in such a case, the use of a symmetric function as in Eq. (5) does not lead to an unbiased estimator anymore.

Following [19], of all unbiased estimators of variance, the only one that is symmetric and has minimum variance is

$$\text{Var}(u_h) \approx \hat{h}_2^{\text{MC}}(u_{h,N}) = \frac{NS_2 - S_1^2}{N(N-1)}. \quad (15)$$

This estimator is known as the second h-statistic [9, 29]. As this satisfies the third condition listed in the previous section, we consider $\hat{\zeta}_m(u_{h,N}) := \hat{h}_2^{\text{MC}}(u_{h,N})$ as the estimated normalizing function. In Eq. (15), S_1 and S_2 are the power sums, given as $S_r \equiv S_r(u_{h,N}) := \sum_{i=1}^N u_h(\omega_i)^r$ for $r = 1, 2$. Therefore, rewriting Eq. (13), where $\text{Var}(u_h)$ is estimated by \hat{h}_2^{MC} as

$$\hat{\varepsilon}(\hat{\mu}^{\text{MC}}) = \frac{e(\hat{\mu}^{\text{MC}})}{\sqrt{\hat{\zeta}_m(u_{h,N})}}, \quad (16)$$

one obtains a new formulation on the scale-invariant MSE (from Eq. (14)) in the form:

$$\hat{\varepsilon}(\hat{\mu}^{\text{MC}}) = \frac{1}{N} + \frac{(\mathbb{E}(u_h) - \mathbb{E}(u))^2}{\hat{\zeta}_m(u_{h,N})}. \quad (17)$$

Certainly, the computational complexity of the scale-invariant MC mean estimate is similar to the conventional procedure (as shown in [7, 25]), but it must be redefined with respect to the total NMSE, which is shown below.

Proposition 3.1 *Let us consider $c_\alpha, c_\gamma, \alpha$ and γ as positive constants, and then one may define the error bounds:*

$$(i) \quad \frac{|\mathbb{E}(u_h) - \mathbb{E}(u)|}{\sqrt{\zeta_m(u_h)}} \leq c_\alpha h^\alpha, \\ (ii) \quad \mathcal{C}(u_h) \leq c_\gamma h^{-\gamma}.$$

Note that, here, the second relation denotes the cost of computing one sample of $u_{h,N}$. Then, for any $0 < \hat{\varepsilon} < e^{-1}$, the MC mean estimator $\hat{\mu}^{\text{MC}}$ with $N = \mathcal{O}(\hat{\varepsilon}^{-2})$ and $h = \mathcal{O}(\hat{\varepsilon}^{-1/\alpha})$ satisfies the NMSE $\hat{\varepsilon}(\hat{\mu}^{\text{MC}}) < \hat{\varepsilon}^2$. Therefore, the corresponding computational cost is given as

$$\mathcal{C}(\hat{\mu}^{\text{MC}}) = N \mathcal{C}(u_h) \leq c \hat{\varepsilon}^{-2-\gamma/\alpha},$$

where, $c > 0$.

3.2 Monte Carlo estimation of variance

The previously derived estimate in Eq. (15) is characterised by an approximation error given as

$$e(\widehat{h}_2^{\text{MC}}) = \widehat{h}_2^{\text{MC}} - \mathbb{V}\text{ar}(u_h) + \mathbb{V}\text{ar}(u_h) - \mathbb{V}\text{ar}(u), \quad (18)$$

in which $\mathbb{V}\text{ar}(u)$ denotes the exact variance of the solution u . Following this, the MSE of the variance estimator reads:

$$\begin{aligned} \varepsilon(\widehat{h}_2^{\text{MC}}) &:= \mathbb{E}(e^2) = \mathbb{E}((\widehat{h}_2^{\text{MC}} - \mathbb{V}\text{ar}(u_h) + \mathbb{V}\text{ar}(u_h) - \mathbb{V}\text{ar}(u))^2) \\ &= \mathbb{E}((\widehat{h}_2^{\text{MC}} - \mathbb{V}\text{ar}(u_h))^2) + (\mathbb{V}\text{ar}(u_h) - \mathbb{V}\text{ar}(u))^2 + \\ &\quad 2(\mathbb{V}\text{ar}(u_h) - \mathbb{V}\text{ar}(u))(\mathbb{E}(\widehat{h}_2^{\text{MC}}) - \mathbb{V}\text{ar}(u_h)). \end{aligned} \quad (19)$$

Having that $\widehat{h}_2^{\text{MC}}$ is an unbiased estimator, meaning that $\mathbb{E}(\widehat{h}_2^{\text{MC}}) = \mathbb{V}\text{ar}(u_h)$, one may further rewrite the previous equation to

$$\varepsilon(\widehat{h}_2^{\text{MC}}) = \mathbb{V}\text{ar}(\widehat{h}_2^{\text{MC}}) + (\mathbb{V}\text{ar}(u_h) - \mathbb{V}\text{ar}(u))^2, \quad (20)$$

in which the first and second terms are the sampling $\varepsilon_s(\widehat{h}_2^{\text{MC}})$ and the square of discretization errors $\varepsilon_d(\widehat{h}_2^{\text{MC}}) = \mathbb{V}\text{ar}(u_h) - \mathbb{V}\text{ar}(u)$, respectively. In the previous equation, the variance of the second-order statistic is derived by [6] and reads

$$\mathbb{V}\text{ar}(\widehat{h}_2^{\text{MC}}) := \frac{1}{N} \left(\mu_4(u_h) - \frac{\mu_2(u_h)^2(N-3)}{(N-1)} \right), \quad (21)$$

where $\mu_2(u_h)$ and $\mu_4(u_h)$ represent the second and fourth central population moments, respectively. For brevity, one may further rewrite the previous equation as

$$\mathbb{V}\text{ar}(\widehat{h}_2^{\text{MC}}) := \frac{\mathbb{V}_2(u_h)}{N}, \quad (22)$$

where

$$\mathbb{V}_2(u_h) := \mu_4(u_h) - \frac{\mu_2(u_h)^2(N-3)}{(N-1)}. \quad (23)$$

Consequently, by substituting Eq. (22) in Eq. (20), one obtains

$$\varepsilon(\widehat{h}_2^{\text{MC}}) = \frac{\mathbb{V}_2(u_h)}{N} + (\mathbb{V}\text{ar}(u_h) - \mathbb{V}\text{ar}(u))^2. \quad (24)$$

Similar to Eq. (10), here the first term defines the statistical error, which is inversely proportional to the number of samples N , and the second part represents the square of the discretization error, directly proportional to parameter h .

3.2.1 Scale-invariant error estimator for Monte Carlo variance estimation

As explained in Section 3.1, for any linear transformation of u_h , the MSE in the above equation would change to bi-quadratic form. This is because of the characteristics of entities in Eq. (23):

$$\mu_4(a u_h + b) = a^4 \mu_4(u_h) \quad (25)$$

and

$$\mu_2^2(a u_h + b) = a^4 \mu_2^2(u_h). \quad (26)$$

Therefore, it is clear that

$$\mathbb{V}_2(a u_h + b) = a^4 \mathbb{V}_2(u_h) \quad (27)$$

and also that

$$(\mathbb{V}_2(a u_h + b) - \mathbb{V}_2(a u + b))^2 = a^4 (\mathbb{V}_2(u_h) - \mathbb{V}_2(u))^2. \quad (28)$$

Similar to the standardising function $\zeta_m(u_h)$ in Section 3.1.1, the normalization entity for the MC variance estimation $\zeta_v(u_h) \in \mathbb{R}^+$ must satisfy the condition $\zeta_v(a u_h + b) = a^4 \zeta_v(u_h)$. Also, the other two requirements, i.e., $0 < \zeta_v < \infty$ and ζ_v is an unbiased estimate and of minimum variance, must be met. From Eq. (27), it is clear that $\mathbb{V}_2(u_h)$ holds the first listed requirement, and further assuming that it also follows the second condition, i.e., $0 < \mathbb{V}_2(u_h) < \infty$, we consider $\zeta_v(u_h) = \mathbb{V}_2(u_h)$. Following this, the new error estimate is given by normalizing Eq. (18) in the form:

$$\hat{e} = \frac{e}{\sqrt{\zeta_v(u_h)}}. \quad (29)$$

This further leads to a new scale-invariant MSE of the MC variance estimate

$$\hat{\varepsilon}(\hat{h}_2^{\text{MC}}) := \mathbb{E}(\hat{e}^2) = \frac{1}{N} + \frac{(\mathbb{V}_2(u_h) - \mathbb{V}_2(u))^2}{\zeta_v(u_h)}, \quad (30)$$

in which the first term is the scale-invariant sampling error $\hat{\varepsilon}_s(\hat{h}_2^{\text{MC}})$ and the second term represents the square of the dimensionless discretization error, $\hat{\varepsilon}_d^2(\hat{h}_2^{\text{MC}}) := \varepsilon_d^2 / \zeta_v(u_h)$.

3.2.2 Unbiased estimation of MC variance normalizing function

The quantity $\mathbb{V}_2(u_h)$ in Eq. (30) is analytical and not known. To determine the unbiased estimate of \mathbb{V}_2 , one must obtain unbiased estimates of entities $\mu_4(u_h)$ and $\mu_2(u_h)^2$ in Eq. (23). To this end, the unbiased approximation of the fourth central moment $\mu_4(u_h)$ is computed by the fourth h-statistic [9]:

$$\begin{aligned} \mu_4(u_h) \approx h_4^{\text{MC}}(u_{h,N}) := & \frac{1}{N(N-1)(N-2)(N-3)} \left(-3S_1^4 + 6NS_1^2S_2 \right. \\ & \left. + (9-6N)S_2^2 + (-4N^2+8N-12)S_1S_3 + (N^3-2N^2+3N)S_4 \right), \end{aligned} \quad (31)$$

whereas the unbiased estimator of $\mu_2(u_h)^2$ is the polyache $h_{\{2,2\}}$ according to [37, 29], given as

$$\begin{aligned} \mu_2(u_h)^2 \approx h_{\{2,2\}}^{\text{MC}}(u_{h,N}) := & \frac{1}{N(N-1)(N-2)(N-3)} \left(S_1^4 - 2NS_1^2S_2 \right. \\ & \left. + (N^2-3N+3)S_2^2 + (4N-4)S_1S_3 + (-N^2+N)S_4 \right). \end{aligned} \quad (32)$$

It is to be noted that the estimator of μ_2^2 by the square of the second h-statistic, i.e., $(\hat{h}_2^{\text{MC}})^2$, leads to a biased estimate, whereas only the polyache $h_{\{2,2\}}$, which is unbiased, remains the preferred way. Therefore, by substituting Eqs. (31) and (32) in Eq. (23), one obtains the unbiased estimate: $\hat{\zeta}_v(u_{h,N}) := \hat{\mathbb{V}}_2^{\text{MC}}(u_{h,N})$ —of $\mathbb{V}_2(u_h)$.

Finally, the MSE in Eq. (30) is re-described in the form:

$$\widehat{\varepsilon}(\widehat{h}_2^{\text{MC}}) := \mathbb{E}(\varepsilon^2) = \frac{1}{N} + \frac{(\text{Var}(u_h) - \text{Var}(u))^2}{\widehat{\zeta}_v(u_{h,N})}. \quad (33)$$

Note that the sampling part of the error is fully normalized, which is identical to the stochastic error of the MC mean estimate in Eq. (17).

Proposition 3.2 *Let us consider $c_\alpha, c_\gamma, \alpha$ and γ as positive constants, and then one may define the error bounds:*

$$(i) \quad \frac{|\text{Var}(u_h) - \text{Var}(u)|}{\sqrt{\zeta_v(u_h)}} \leq c_\alpha h^\alpha,$$

$$(ii) \quad \mathcal{C}(u_h) \leq c_\gamma h^{-\gamma}.$$

Then, for any $0 < \varepsilon < e^{-1}$, the MC variance estimator $\widehat{h}_2^{\text{MC}}$ with $N = \mathcal{O}(\varepsilon^{-2})$ and $h = \mathcal{O}(\varepsilon^{-1/\alpha})$ satisfies the NMSE $\widehat{\varepsilon}(\widehat{h}_2^{\text{MC}}) < \varepsilon^2$. Therefore, the corresponding computational cost is given as

$$\mathcal{C}(\widehat{h}_2^{\text{MC}}) \leq c \varepsilon^{-2-\gamma/\alpha}.$$

where, $c > 0$.

Notice that, for a given normalized and estimated deterministic error s.t. $\widehat{\varepsilon}_d(\widehat{\mu}^{\text{MC}}) = \widehat{\varepsilon}_d(\widehat{h}_2^{\text{MC}})$, the computational complexity of the MC variance estimator corresponding to the total NMSE ε^2 remains identical to that of the MC mean.

4 Multilevel Monte Carlo method

The Eqs. (10), (14), (24) and (30) signify that to attain an overall higher level of accuracy, one requires a very fine resolution of the finite element mesh grid and a very large number of MC samples. This demands a tremendous amount of computational effort, making the algorithm practically infeasible. Therefore, the desired moments are further estimated by a variance reduction technique in a multilevel fashion following [20, 14, 15, 10, 7].

4.1 Multilevel Monte Carlo estimation of mean

Let $\{l = 0, 1, 2, \dots, L\}$ be a generalised increasing sequence—in the context of decreasing element size h —of nested mesh-grids \mathcal{P}_l , a regular (non-degenerate) partition of the computational domain \mathcal{G} of the problem described in Eq. (1). Here l denotes the mesh level, and L represents the finest mesh. The goal of the MLMC method is to determine the statistics (such as the mean in this case) of the solution $u_{h_L}(\omega)$ on the finest level L . To this end, by exploiting the linearity of the expectation operator, one may express the MLMC (also denoted by ML) mean estimate of the mean $\mu(u_{h_L})$ using a set of samples $\{N_l\} := \{N_0, N_1, \dots, N_L\}$ as [20]

$$\begin{aligned} \widehat{\mu}^{\text{ML}}(u_{h_L, \{N_l\}}) &:= \widehat{\mu}^{\text{MC}}(u_{h_0, N_0}) + \sum_{l=1}^L \widehat{\mu}^{\text{MC}}(u_{h_l, N_l} - u_{h_{l-1}, N_l}) \\ &= \sum_{l=0}^L \widehat{\mu}^{\text{MC}}(Y_{h_l, N_l}). \end{aligned} \quad (34)$$

Here $\hat{\mu}^{\text{MC}}(u_{h_0, N_0})$ is the MC estimator of mean $\mu(u_{h_0})$ on level $l = 0$ using N_0 samples, and $\hat{\mu}^{\text{MC}}(u_{h_l, N_l} - u_{h_{l-1}, N_{l-1}})$ represents the approximation of mean $\mu(u_{h_l, N_l} - u_{h_{l-1}, N_{l-1}})$ with $l > 0$ and N_l samples. Furthermore, $\mu^{\text{MC}}(Y_{h_l, N_l})$ is the MC estimator of $\mu(Y_{h_l})$ such that for $l = 0$, $Y_{h_0, N_0} = u_{h_0, N_0}$; otherwise, $Y_{h_l, N_l} := u_{h_l, N_l} - u_{h_{l-1}, N_{l-1}}$. Note that each term Y_{h_l, N_l} , $l \geq 0$, is sampled independently, whereas when $l > 0$, the quantities u_{h_l, N_l} and $u_{h_{l-1}, N_{l-1}}$ in Y_{h_l, N_l} are considered to be strongly correlated—meaning that u_{h_l, N_l} and $u_{h_{l-1}, N_{l-1}}$ are sampled from the same random seed.

As the mean estimate on the finest grid $\hat{\mu}^{\text{ML}} \equiv \hat{\mu}^{\text{ML}}(u_{h_L, \{N_l\}})$ is obtained as the telescopic sum of the difference of MC mean estimates on the coarser grids, the MSE corresponding to Eq. (10) takes the form:

$$\varepsilon(\hat{\mu}^{\text{ML}}) = \sum_{l=0}^L \frac{\text{Var}(Y_{h_l})}{N_l} + (\mathbb{E}(u_{h_L}) - \mathbb{E}(u))^2. \quad (35)$$

The above error consists of two terms: the variance of the estimator $\hat{\mu}^{\text{ML}}(u_{h_L, \{N_l\}})$, given as $\varepsilon_s(\hat{\mu}^{\text{ML}})$, and the square of the spatial discretization error, i.e., $\varepsilon_d^2(\hat{\mu}^{\text{ML}}) := (\mathbb{E}(u_{h_L}) - \mathbb{E}(u))^2$.

4.1.1 Scale-invariant multilevel Monte Carlo estimation of mean

Similar to the MC error estimate for the mean in Eq. (10), Eq. (35) depicts a classical absolute error estimate. As a result, the convergence of the MLMC algorithm strongly depends on the solution magnitude. Hence, by assuming $\zeta_m(u_{h_L}) = \text{Var}(u_{h_L})$ as a standardising function (the properties of which are listed in Section 3.1.1), we suggest a new scale-invariant MSE estimate following Eq. (13):

$$\hat{\varepsilon}(\hat{\mu}^{\text{ML}}) = \frac{1}{\zeta_m(u_{h_L})} \left(\sum_{l=0}^L \frac{\text{Var}(Y_{h_l})}{N_l} \right) + \frac{(\mathbb{E}(u_{h_L}) - \mathbb{E}(u))^2}{\zeta_m(u_{h_L})}. \quad (36)$$

However, the normalization term $\text{Var}(u_{h_L})$ here is generally not known. Hence, under the assumption that for any value of l , $\text{Var}(u_{h_l})$ will be approximately constant [15, 7], one may substitute $\zeta_m(u_{h_L}) = \text{Var}(u_{h_L})$ with $\zeta_m(u_{h_0}) = \text{Var}(u_{h_0})$. Furthermore, under the consideration that $\hat{\zeta}_m(u_{h_0, N_0}) := \hat{h}_2^{\text{MC}}(u_{h_0, N_0})$ is the MC estimator of $\text{Var}(u_{h_0})$, and by defining the MC variance estimate of $\text{Var}(Y_{h_l}) := \text{Var}(u_{h_l} - u_{h_{l-1}})$ via $\hat{h}_2^{\text{MC}}(Y_{h_l, N_l})$, Eq. (36) therefore transforms to

$$\hat{\varepsilon}(\hat{\mu}^{\text{ML}}) = \frac{1}{\hat{\zeta}_m(u_{h_0, N_0})} \left(\sum_{l=0}^L \frac{\hat{h}_2^{\text{MC}}(Y_{h_l, N_l})}{N_l} \right) + \frac{(\mathbb{E}(u_{h_L}) - \mathbb{E}(u))^2}{\hat{\zeta}_m(u_{h_0, N_0})}. \quad (37)$$

The first entity here stands for the estimated scale-invariant multi-level sampling error $\hat{\varepsilon}_s(\hat{\mu}^{\text{ML}})$, whereas the second term defines the square of the dimensionless discretization error $\hat{\varepsilon}_d^2(\hat{\mu}^{\text{ML}})$. Therefore, to attain an overall normalized mean square error (NMSE) $\hat{\varepsilon}^2$, it is adequate, for instance, to satisfy conditions such as $\hat{\varepsilon}_s(\hat{\mu}^{\text{ML}}) < \hat{\varepsilon}^2/2$ and $\hat{\varepsilon}_d^2(\hat{\mu}^{\text{ML}}) < \hat{\varepsilon}^2/2$. Note that the equal splitting of $\hat{\varepsilon}^2$ is not a requirement and can also be set otherwise—for more information on this, see [18].

If $\mathcal{C}_l \equiv \mathcal{C}(Y_{h_l, N_l})$ is the computational cost of determining a single MC sample of Y_{h_l, N_l} , then the overall cost of the estimator $\hat{\mu}^{\text{ML}}$ is given as $\mathcal{C}(\hat{\mu}^{\text{ML}}) := \sum_{l=0}^L N_l \mathcal{C}_l$. Here, the

optimum number of samples N_l on each level l is evaluated by solving an optimisation problem such that the condition $\hat{\epsilon}_s < \epsilon^2/2$ is satisfied. As a result, the cost function

$$f(N_l) = \arg \min_{N_l} \sum_{l=0}^L \left(N_l \mathcal{C}_l + \tau \frac{\hat{h}_2^{\text{MC}}(Y_{h_l, N_l})}{\hat{\zeta}_m(u_{h_0, N_0}) N_l} \right) \quad (38)$$

is minimised, due to which the optimal samples N_l are calculated as

$$N_l = \tau \left(\frac{\hat{h}_2^{\text{MC}}(Y_{h_l, N_l})}{\hat{\zeta}_m(u_{h_0, N_0}) \mathcal{C}_l} \right)^{\frac{1}{2}}. \quad (39)$$

Here, τ is the Lagrange multiplier, determined by

$$\tau \geq \frac{2}{\epsilon^2} \sum_{l=0}^L \left(\frac{\hat{h}_2^{\text{MC}}(Y_{h_l, N_l}) \mathcal{C}_l}{\hat{\zeta}_m(u_{h_0, N_0})} \right)^{\frac{1}{2}}. \quad (40)$$

On the other hand, the set of meshlevels $\{l = 0, 1, 2, \dots, L\}$ maybe optimally chosen (in a geometric or non-geometric sequence) for a given deterministic error s.t. $\hat{\epsilon}_d^2 < \epsilon^2/2$. Typically, for PDE-based applications, the choice of coarse mesh $l = 0$ depends on the regularity of the solution $u(x)$ [7]. Following this, the finer mesh selection is based on an apriori mesh convergence study, where the finest mesh grid $l = L$ can be fixed or can be adaptively selected [15] during the MLMC mean computation. For a more detailed discussion on the optimal selection of mesh hierarchies, see [18].

The arguments for determining the total computational cost of the MLMC mean estimator follow the classical MLMC procedure; for example, see [14, 20]. However, the difference is that the cost is described with respect to a given NMSE instead of the MSE.

Proposition 4.1 *Let us consider the positive constants $c_\alpha, c_\beta, c_\gamma, \alpha, \beta, \gamma$, given that $\alpha \geq \frac{1}{2} \min(\beta, \gamma)$ and assume that the following error bounds*

$$\begin{aligned} (i) \quad & \frac{|\mathbb{E}(u_{h_l}) - \mathbb{E}(u)|}{\sqrt{\zeta_m(u_h)}} \leq c_\alpha h_l^\alpha, \\ (ii) \quad & \frac{\hat{h}_2^{\text{MC}}(Y_{h_l, N_l})}{\zeta_m(u_h)} \leq c_\beta h_l^\beta, \\ (iii) \quad & \mathcal{C}_l \leq c_\gamma h_l^{-\gamma} \end{aligned} \quad (41)$$

hold. Then, there exists another positive constant c , such that for any $0 < \epsilon < e^{-1}$, the MLMC normalized mean square error estimator satisfies $\hat{\epsilon}(\hat{\mu}^{\text{ML}}) < \epsilon^2$, and the total computational cost is bound by

$$\mathcal{C}(\hat{\mu}^{\text{ML}}) \leq \begin{cases} c \epsilon^{-2}, & \beta > \gamma, \\ c \epsilon^{-2(\log \epsilon)^2}, & \beta = \gamma, \\ c \epsilon^{-2-(\gamma-\beta)/\alpha}, & \beta < \gamma. \end{cases}$$

Based on the values of β and γ , one may also understand the major cost contributor amongst the sequence of mesh grids. If $\beta > \gamma$, the maximum cost is controlled by the coarsest level, and if $\beta < \gamma$, the finest level governs the dominant cost. Finally, when $\beta = \gamma$, the cost at each level is roughly evenly distributed.

Furthermore, it is clear for the first relation in Eq. (41) that as $l \rightarrow \infty$,

$$\frac{|\mathbb{E}(u_{h_l}) - \mathbb{E}(u)|}{\sqrt{\zeta_m(u_h)}} \rightarrow 0.$$

However, $\mathbb{E}(u)$ is analytical and not known. Therefore, the deterministic error is defined via the triangle inequality as [7]

$$\frac{|\hat{\mu}^{\text{MC}}(Y_{h_l, N_l})|}{\sqrt{\zeta_m(u_h)}} \leq c_\alpha h_l^\alpha. \quad (42)$$

4.2 Multilevel Monte Carlo estimation of variance

To enhance the characterization of the probabilistic system response $u_{h_L}(\omega)$, this paper also focuses on defining the MLMC estimator of $\mathbb{V}\text{ar}(u_{h_L})$ using h-statistics [25], expressed in the form:

$$\hat{h}_2^{\text{ML}}(u_{h_L, \{N_l\}}) := \hat{h}_2^{\text{MC}}(u_{h_0, N_0}) + \sum_{l=1}^L \left(\hat{h}_2^{\text{MC}}(u_{h_l, N_l}) - \hat{h}_2^{\text{MC}}(u_{h_{l-1}, N_l}) \right). \quad (43)$$

Here $\hat{h}_2^{\text{MC}}(u_{h_0, N_0})$ is the MC estimator of $\mathbb{V}\text{ar}(u_{h_0})$ with N_0 samples; $\hat{h}_2^{\text{MC}}(u_{h_l, N_l})$ and $\hat{h}_2^{\text{MC}}(u_{h_{l-1}, N_l})$ represent the MC estimation of $\mathbb{V}\text{ar}(u_{h_l})$ and $\mathbb{V}\text{ar}(u_{h_{l-1}})$ using N_l samples, respectively. For simplification, we introduce:

$$Z_{h_l, N_l} = \begin{cases} \hat{h}_2^{\text{MC}}(u_{h_0, N_0}), & l = 0, \\ \hat{h}_2^{\text{MC}}(u_{h_l, N_l}) - \hat{h}_2^{\text{MC}}(u_{h_{l-1}, N_l}), & l > 0. \end{cases} \quad (44)$$

Note that, for $l > 0$, u_{h_l, N_l} and u_{h_{l-1}, N_l} in Z_{h_l, N_l} are determined using the same random seed. Thus, the expansion in Eq. (43) is rewritten as

$$\hat{h}_2^{\text{ML}} = \sum_{l=0}^L Z_{h_l, N_l}. \quad (45)$$

In correspondence to Eq. (19), the MSE of the estimator \hat{h}_2^{ML} takes the form:

$$\varepsilon(\hat{h}_2^{\text{ML}}) = \mathbb{V}\text{ar}\left(\hat{h}_2^{\text{ML}}\right) + (\mathbb{V}\text{ar}(u_{h_L}) - \mathbb{V}\text{ar}(u))^2. \quad (46)$$

Under further consideration that the quantity Z_{h_l, N_l} , for $l \geq 0$, is sampled independently, one may express the first term in the above equation as

$$\mathbb{V}\text{ar}\left(\hat{h}_2^{\text{ML}}\right) = \sum_{l=0}^L \mathbb{V}\text{ar}(Z_{h_l, N_l}), \quad (47)$$

in which the variance $\mathbb{V}\text{ar}(Z_{h_l, N_l})$ is further defined—similar to Eq. (22)—by $\mathbb{V}_{l,2}/N_l$. Therefore, Eq. (46) is reformulated as

$$\varepsilon(\hat{h}_2^{\text{ML}}) = \sum_{l=0}^L \frac{\mathbb{V}_{l,2}}{N_l} + (\mathbb{V}\text{ar}(u_{h_L}) - \mathbb{V}\text{ar}(u))^2. \quad (48)$$

Analogous to Eq. (10), the MSE in Eq. (48) is split into statistical error $\varepsilon_s(\widehat{h}_2^{\text{ML}})$ —which is of the order $\mathcal{O}(N_l^{-1})$ —and square of deterministic bias, $\varepsilon_d^2(\widehat{h}_2^{\text{ML}}) := (\mathbb{V}\text{ar}(u_{h_L}) - \mathbb{V}\text{ar}(u_h))^2$.

Following the notion of power sum S_r defined in Section 3.1, here we introduce the bivariate power sum [29, 25]

$$S_l^{a,b} := \sum_{i=1}^N X_{h_l}^+(\omega_i)^a X_{h_l}^-(\omega_i)^b, \quad (49)$$

where $X_{h_l}^+(\omega_i)_{i=1,\dots,N_l} := X_{h_l, N_l}^+ = u_{h_l, N_l} + u_{h_{l-1}, N_l}$ and $X_{h_l}^-(\omega_i)_{i=1,\dots,N_l} := X_{h_l, N_l}^- = u_{h_l, N_l} - u_{h_{l-1}, N_l}$. Subsequently, the unbiased MC estimation of the quantity $\mathbb{V}_{l,2}$ in Eq. (47) reads:

$$\begin{aligned} \widehat{\mathbb{V}}_{l,2}^{\text{MC}} = & \frac{1}{(N_l - 3)(N_l - 2)(N_l - 1)^2 N_l} \left(N_l \left((-N_l^2 + N_l + 2)(S_l^{1,1})^2 \right. \right. \\ & + (N_l - 1)^2 (N_l S_l^{2,2} - 2S_l^{1,0} S_l^{1,2}) + (N_l - 1) S_l^{0,2} ((S_l^{1,0})^2 - S_l^{2,0}) \\ & + (S_l^{0,1})^2 \left((6 - 4N_l)(S_l^{1,0})^2 + (N_l - 1) N_l S_l^{2,0} \right) - \\ & \left. \left. 2N_l S_l^{0,1} \left((N_l - 1)^2 S_l^{2,1} + (5 - 3N_l) S_l^{1,0} S_l^{1,1} \right) \right). \end{aligned} \quad (50)$$

4.2.1 Scale-invariant multilevel Monte Carlo estimation of variance

As described in Eq. (30), the MSE in Eq. (48) is transformed to a scale-invariant version $\widehat{\varepsilon}(\widehat{h}_2^{\text{ML}})$ by considering $\zeta_v(u_{h_L}) = \mathbb{V}_2(u_{h_L})$ as the normalization entity, which is unknown. Therefore, we make the assumption that the value of $\mathbb{V}_2(u_{h_L})$ stays approximately close for all values of l , i.e., $\mathbb{V}_2(u_{h_L}) \approx \mathbb{V}_2(u_{h_0})$. Following this, if $\widehat{\zeta}_v(u_{h_0, N_0}) := \widehat{\mathbb{V}}_2^{\text{MC}}(u_{h_0, N_0})$ is the MC estimator of $\mathbb{V}_2(u_{h_0})$, then the new normalized MSE is given in the form:

$$\widehat{\varepsilon}(\widehat{h}_2^{\text{ML}}) = \frac{1}{\widehat{\zeta}_v(u_{h_0, N_0})} \left(\sum_{l=0}^L \frac{\widehat{\mathbb{V}}_{l,2}^{\text{MC}}}{N_l} \right) + \frac{(\mathbb{V}\text{ar}(u_{h_L}) - \mathbb{V}\text{ar}(u))^2}{\widehat{\zeta}_v(u_{h_0, N_0})}, \quad (51)$$

in which the first term defines the scale-invariant sampling error $\widehat{\varepsilon}_s(\widehat{h}_2^{\text{ML}})$ and the second term is the square of the normalized deterministic error $\widehat{\varepsilon}_d^2(\widehat{h}_2^{\text{ML}})$. The accomplishment of a total NMSE $\widehat{\varepsilon}^2$ —as mentioned in Section 4.1.1—is justified by ensuring that both errors are less than $\widehat{\varepsilon}^2/2$.

One may determine the samples N_l analogously to Eqs. (38)-(40):

$$N_l = \frac{2}{\widehat{\varepsilon}^2} \sum_{l=0}^L \left(\frac{\widehat{\mathbb{V}}_{l,2}^{\text{MC}} \mathcal{C}_l}{\widehat{\zeta}_v(u_{h_0, N_0})} \right)^{\frac{1}{2}} \left(\frac{\widehat{\mathbb{V}}_{l,2}^{\text{MC}}}{\widehat{\zeta}_v(u_{h_0, N_0}) \mathcal{C}_l} \right)^{\frac{1}{2}}. \quad (52)$$

Note that here \mathcal{C}_l is the computational cost of evaluating one MC sample of u_{h_l, N_l} and u_{h_{l-1}, N_l} in the difference term Z_{h_l, N_l} , which is equivalent to determining the cost of Y_{h_l, N_l} in Eq. (38). Following the computational complexity of the scale-invariant MLMC mean in Proposition 4.1, the computing cost of the normalized MLMC variance estimate is also similar to the conventional MLMC variance (see [25, 3]), which is detailed below.

Proposition 4.2 *Let us introduce the positive constants $c_\alpha, c_\beta, c_\gamma, \alpha, \beta, \gamma$, such that $\alpha \geq \frac{1}{2} \min(\beta, \gamma)$ and the error bounds*

$$\begin{aligned}
(i) \quad & \frac{|\text{Var}(u_{h_l}) - \text{Var}(u)|}{\sqrt{\zeta_v(u_h)}} \leq c_\alpha h_l^\alpha, \\
(ii) \quad & \frac{\widehat{\mathbb{V}}_{l,2}^{MC}}{\zeta_v(u_h)} \leq c_\beta h_l^\beta, \\
(iii) \quad & \mathcal{C}_l \leq c_\gamma h_l^{-\gamma},
\end{aligned} \tag{53}$$

are satisfied. Thus, one may state that, for any $0 < \hat{\epsilon} < e^{-1}$, the total NMSE is bound by $\widehat{\hat{\epsilon}}(\widehat{h}_2^{ML}) < \hat{\epsilon}^2$ with a computational cost

$$\mathcal{C}(\widehat{h}_2^{ML}) \leq \begin{cases} c \hat{\epsilon}^{-2}, & \beta > \gamma, \\ c \hat{\epsilon}^{-2(\log \hat{\epsilon})^2}, & \beta = \gamma, \\ c \hat{\epsilon}^{-2-(\gamma-\beta)/\alpha}, & \beta < \gamma. \end{cases} \tag{54}$$

Here, $c > 0$ is a constant.

Notably, if the first and second assumptions in Eqs. (41) and (53) are correspondingly equal, then the computational complexity of the MLMC variance estimator will be asymptotically equal to that of the mean estimate. However, this depends on the regularity of solution $u(x, \omega)$, as stated in [3]. Otherwise, generally, for a given NMSE $\hat{\epsilon}^2$, the mean estimator runs faster as compared to the variance (to be elaborated further with an example in Section 6).

Furthermore, as noted in Section 4.1, mesh level $l = 0$ contributes the most cost in the first scenario in the Eq. (54); the second case imposes an almost equal cost on all mesh grids, and the final relation demonstrates that the finest level L is the most dominant.

Also, corresponding to Eq. (53), when $l \rightarrow \infty$, there is a monotonic decay in $|\text{Var}(u_{h_l}) - \text{Var}(u)|/\sqrt{\zeta_v(u_h)}$. Thereby, analogous to Eq. (42), the following condition

$$\frac{|\text{Var}(u_{h_l}) - \text{Var}(u_{h_{l-1}})|}{\sqrt{\zeta_v(u_h)}} \leq c_\alpha h_l^\alpha. \tag{55}$$

5 Application to linear elasticity: a model problem

5.1 Deterministic setting: linear elasticity

Let $\mathcal{G} \subset \mathbb{R}^d$ be a d -dimensional geometry with smooth Lipschitz boundary Γ . The aim is to determine the displacement vector $\mathbf{u} \in \mathbb{R}^d$ (which belongs to the Hilbert space \mathcal{U}) at a spatial point $\mathbf{x} \in \mathcal{G}$ that completely satisfy the equilibrium equations

$$\begin{aligned}
-\text{div } \boldsymbol{\sigma}(\mathbf{x}) &= \mathbf{f}(\mathbf{x}), \quad \forall \mathbf{x} \in \mathcal{G}, \\
\mathbf{u}(\mathbf{x}) &= \mathbf{u}_0 = \mathbf{0}, \quad \forall \mathbf{x} \in \Gamma_D, \\
\boldsymbol{\sigma}(\mathbf{x}) \cdot \mathbf{n}(\mathbf{x}) &= \mathbf{t}(\mathbf{x}), \quad \forall \mathbf{x} \in \Gamma_N,
\end{aligned} \tag{56}$$

describing the linear-elastic behaviour. Here, $\boldsymbol{\sigma}(\mathbf{x})$ is the Cauchy stress tensor, which belongs to the space of second-order symmetric tensors $\text{Sym}(d) :=$

$\{\boldsymbol{\sigma} \in (\mathbb{R}^d \otimes \mathbb{R}^d) \mid \boldsymbol{\sigma} = \boldsymbol{\sigma}^T\}$; $\mathbf{f}(x) \in \mathbb{R}^d$ is the body force; $\mathbf{t}(x) \in \mathbb{R}^d$ represents the surface tension on the Neumann boundary $\Gamma_N \subset \Gamma$, and $\mathbf{n}(\mathbf{x}) \in \mathbb{R}^d$ is the outward unit normal to Γ_N . For simplicity, a homogeneous boundary condition $\mathbf{u}_0 = \mathbf{0} \in \mathbb{R}^d$ is considered on the Dirichlet boundary $\Gamma_D \subset \Gamma$. It is also possible to assume that $\Gamma_D \cap \Gamma_N = \emptyset$.

One may further describe the strain-displacement relation as

$$\boldsymbol{\varepsilon}(x) = \frac{1}{2} (\nabla \mathbf{u} + \nabla \mathbf{u}^T), \quad \forall \mathbf{x} \in \mathcal{G}, \quad (57)$$

where $\boldsymbol{\varepsilon}(x) \in \text{Sym}(d)$ denotes an infinitesimal second-order symmetric strain tensor. Finally, the material constitutive equation is of the linear form

$$\boldsymbol{\sigma}(x) = \mathbf{C}(\mathbf{x}) : \boldsymbol{\varepsilon}(x), \quad \forall \mathbf{x} \in \mathcal{G}, \quad (58)$$

in which $\mathbf{C}(\mathbf{x})$ represents a spatially varying fourth-order positive-definite symmetric elasticity tensor. Here, the notion of symmetry signifies the major ($C_{ijkl} = C_{klij}$) and minor symmetries ($C_{ijkl} = C_{jikl} = C_{ijlk}$). As a result, one can map a $\mathbf{C}(\mathbf{x})$ tensor to a second-order tensor $C(\mathbf{x})$, more generally known as the elasticity matrix. The reduced $C(\mathbf{x})$ matrix belongs to a family of $(n \times n)$, where $n = d(d+1)/2$, real-valued positive-definite symmetric matrices:

$$\text{Sym}^+(n) = \{C \in (\mathbb{R}^n \otimes \mathbb{R}^n) \mid C = C^T, \mathbf{z}^T C \mathbf{z} > 0, \forall \mathbf{z} \in \mathbb{R}^n \setminus \mathbf{0}\}. \quad (59)$$

Accordingly, conforming to Voigt notation, Eq. (58) transforms to $\boldsymbol{\sigma}(\mathbf{x}) = C(\mathbf{x}) \cdot \boldsymbol{\varepsilon}(\mathbf{x})$, with $\boldsymbol{\sigma}(\mathbf{x}) \in \mathbb{R}^d$ and $\boldsymbol{\varepsilon}(\mathbf{x}) \in \mathbb{R}^d$ denoting the stress and strain vectors, respectively.

5.2 Reduced parametric modelling of material uncertainty

Material law as described previously is complicated when highly heterogeneous and anisotropic materials—such as bone tissue, see Section 6—are to be modelled. To include aleatoric uncertainty with heterogeneity in Eq. (58), the material properties have to be modelled as random and spatially dependent. In this paper, a probabilistic point of view is studied, in which the $C(\mathbf{x})$ matrix is modelled as a matrix-valued second-order random field $C(\mathbf{x}, \omega)$ on a probability space $(\Omega, \mathcal{F}, \mathbb{P})$. In other words, the random elasticity matrix can be modelled as a mapping:

$$C(\mathbf{x}, \omega) : \mathcal{G} \times \Omega \rightarrow \text{Sym}^+(n). \quad (60)$$

Furthermore, in practise, the usual assumption is that the elasticity matrix $C(\mathbf{x})$ globally follows a certain type of symmetry (e.g., isotropic, orthotropic, etc.; see [8, 5] for invariance classification of elasticity matrix C), even though the experiments today cannot provide this information with full certainty. Therefore, to include uncertainty in the type of material symmetry, in this paper, we model the elasticity matrix $C(\mathbf{x})$ as per the reduced parametric approach (also commonly known as the non-parametric method) [32, 33, 17]. That is, the random matrix $C(\mathbf{x}, \omega)$ follows a specific type of symmetry only in the mean, whereas each of the realisations belongs to the triclinic system, which is the lowest order of symmetry for elasticity-type tensors. This gives our model a full degree of freedom in a case where the predefined mean symmetry turns out to be incorrect; one would still be able to identify other types of invariances given experimental data. This is, however, not the case if we assume that each of the realisations is constrained.

Following this, we model the homogeneous mean matrix as $\mathbb{E}(C(\mathbf{x}, \omega)) = Q^T Q$, in which the term $Q \in \mathbb{R}^{n \times n}$ represents an upper triangular matrix—this square-type (Cholesky) factorization ensures the positive-definiteness of the mean matrix. Then, to allow uncertainty into the model, the mean formulation is extended to

$$C(\mathbf{x}, \omega) = Q^T T(\mathbf{x}, \omega) Q, \quad (61)$$

such that

$$\mathbb{E}(T(\mathbf{x}, \omega)) = I \quad (62)$$

holds. Here, $T(\mathbf{x}, \omega)$ is a matrix-valued random variable that also resides in $\text{Sym}^+(n)$, the mean value of which is an identity matrix $I \in \text{Sym}^+(n)$. In this manner, the mean behaviour is controlled by $\mathbb{E}(C(\mathbf{x}, \omega))$, and the random fluctuations are governed by $T(\mathbf{x}, \omega)$. To construct a random ensemble $T(\mathbf{x}, \omega)$, one may use the maximum entropy optimisation principle under the constraints mentioned in the previous list (but with a mean defined in Eq. (62)). Henceforth, $T(\mathbf{x}, \omega)$ can further be factorised as

$$T(\mathbf{x}, \omega) = U(\mathbf{x}, \omega)^T U(\mathbf{x}, \omega), \quad (63)$$

and by substitution in Eq. (61), one obtains

$$C(\mathbf{x}, \omega) = Q^T U(\mathbf{x}, \omega)^T U(\mathbf{x}, \omega) Q. \quad (64)$$

Here, $U(\mathbf{x}, \omega) \in \mathbb{R}^{n \times n}$ denotes the upper triangular random matrix with entries

$$V_{ij} = \begin{cases} \frac{\delta_T}{\sqrt{d+1}} \theta_{ij}(\mathbf{x}, \omega), & \text{if } i < j \\ \frac{\delta_T}{\sqrt{d+1}} \sqrt{N_c \Gamma_{\alpha_j}(\mathbf{x}, \omega)}, & \text{if } i = j, \end{cases} \quad (65)$$

given that the elements $V_{ij}, i \leq j$ are independent. Observe that the non-diagonal upper triangular elements are modelled as independent Gaussian random fields $\theta_{ij}(\mathbf{x}, \omega), 1 \leq i \leq j \leq n$ with zero mean and unit variance. On the other hand, the diagonal entries are gamma-distributed positive-definite random fields:

$$\Gamma_{\alpha_j}(\mathbf{x}, \omega) = F_{\Gamma_{\alpha}}^{-1} \circ \text{erf}(\theta_{ij}(\mathbf{x}, \omega)). \quad (66)$$

Here,

$$\alpha_j = (d+1)/(2\delta_T^2) + (1-j)/2 \quad (67)$$

is a positive real number; erf is the standard Gaussian distribution function; and $F_{\Gamma_{\alpha}}^{-1}$ is the inverse gamma cumulative distribution function. This assures that the diagonal elements are strictly positive, and therefore, the random matrix $T(\mathbf{x}, \omega)$ also remains positive-definite. Reverting to the above description in Eq. (65), where N_c is a normalisation constant of the resultant function (given in Eq. (66)), the value of which equals 2. Furthermore, $\delta_T := [0, 1] \in \mathbb{R}$ defined as Eq. (68), is a scalar value that controls the dispersion of $T(\mathbf{x}, \omega)$:

$$\delta_T = \left\{ \frac{1}{d} \mathbb{E} \left[\| T(\mathbf{x}, \omega) - I \|^2 \right] \right\}^{1/2}. \quad (68)$$

The coefficient of dispersion parameter δ_T is chosen such that

$$\delta_C = \left[\frac{\mathbb{E} \{ \| C(\mathbf{x}, \omega) - \mathbb{E}(C(\mathbf{x}, \omega)) \|^2 \}}{\| \mathbb{E}(C(\mathbf{x}, \omega)) \|^2} \right]^{1/2} = \frac{\delta_T}{\sqrt{d+1}} \left[1 + \frac{(\text{tr}(\mathbb{E}(C(\mathbf{x}, \omega))))^2}{\text{tr}(\mathbb{E}(C(\mathbf{x}, \omega)))^2} \right]^{1/2} \quad (69)$$

holds. Here, $\delta_C := [0, 1] \in \mathbb{R}$ is the coefficient of dispersion of the random matrix $C(\mathbf{x}, \omega)$.

5.3 Stochastic setting: linear elasticity

The description of the random elasticity matrix field $C(\mathbf{x}, \omega)$ leads to the apparent transformation of a linear-elastic material model to a stochastic model. The aim is to determine the random displacement vector field $\mathbf{u}(\mathbf{x}, \omega) : \mathcal{G} \times \Omega \rightarrow \mathbb{R}^d$. Therefore, the equilibrium equations are rewritten in the form

$$\begin{aligned} -\operatorname{div} \boldsymbol{\sigma}(\mathbf{x}, \omega) &= \mathbf{f}(x), \quad \forall x \in \mathcal{G}, \omega \in \Omega, \\ \mathbf{u}(x, \omega) &= \mathbf{u}_0 = \mathbf{0}, \quad \forall x \in \Gamma_D, \omega \in \Omega, \\ \boldsymbol{\sigma}(x, \omega) \cdot \mathbf{n}(x) &= \mathbf{t}(x), \quad \forall x \in \Gamma_N, \omega \in \Omega, \end{aligned} \quad (70)$$

in which the boundary conditions and body forces $\mathbf{f}(x)$ remain deterministic. Further, the linearized kinematics relationship is transformed to

$$\boldsymbol{\varepsilon}(x, \omega) = \frac{1}{2} \left(\nabla \mathbf{u}(x, \omega) + \nabla \mathbf{u}(x, \omega)^T \right), \quad \forall x \in \mathcal{G}, \omega \in \Omega, \quad (71)$$

where the $\nabla(\cdot)$ operator is taken in a weak sense. Finally, the constitutive law is represented by

$$\boldsymbol{\sigma}(x, \omega) = \mathbf{C}(x, \omega) : \boldsymbol{\varepsilon}(x, \omega), \quad \forall x \in \mathcal{G}, \omega \in \Omega. \quad (72)$$

By carrying out the variational formulation of the above stochastic partial differential equations on \mathcal{G} and further discretizing in a finite element setting, one searches for the solution $\mathbf{u}_h(\mathbf{x}, \omega) : \mathcal{U}_h \times \Omega \rightarrow \mathbb{R}^d$ in a finite subspace, \mathcal{U}_h , as described in [30, 22]. More precisely, the goal of this study is to determine the total displacement scalar field in Euclidean norm, i.e., $u_h^{(t)}(\mathbf{x}, \omega) = \|\mathbf{u}_h(\mathbf{x}, \omega)\|$, and estimate the second-order statistics such as the mean and variance of sampled response $u_{h,N}^{(t)} := [u_h^{(t)}(\mathbf{x}, \omega_i)]_{i=1}^N$ using the scale-invariant MC and MLMC as detailed in Sections (3) and (4).

6 Numerical results: 2D human femur

6.1 Specifications

A two-dimensional proximal femur bone geometry with a body width of approximately 7cm and 21.7cm in total height is considered. Fig. 1 shows the boundary conditions where an in-plane uniform pressure load with a resultant load of 1500N is applied on top of the bone and zero displacements are considered at the bottom [39]. The finite element method (FEM) based spatial discretization is undergone using four-noded plane stress elements. By sampling the probabilistic space, each deterministic simulation is thus executed by the finite element MATLAB-based solver Plaston [30].

To implement the scale-invariant MLMC method, a sequence of four nested meshes with element size $h_{l-1} = 2h_l$ are considered, as shown in Fig. 2. One may notice the identical implementation of boundary conditions over all the mesh levels. The corresponding mesh specifications are tabulated in Table 1. To this end, a matrix-valued random field $C(\mathbf{x}, \omega)$, as

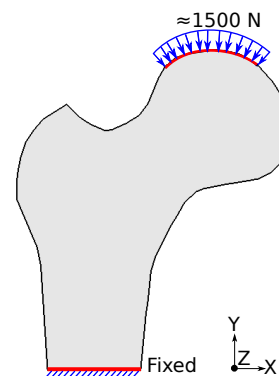


Figure 1: Geometry and boundary conditions

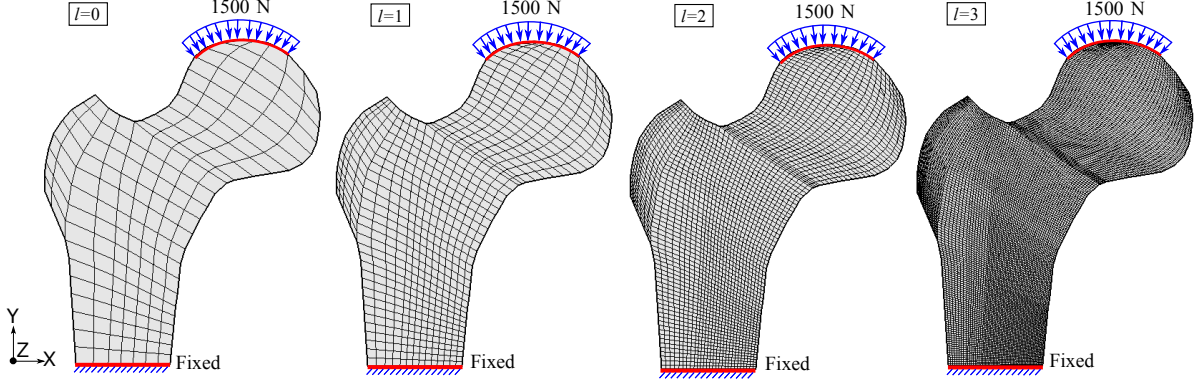


Figure 2: Nested mesh grids of 2D femur bone

described in Eq. (61), is modelled. A homogeneous mean matrix $\mathbb{E}(C(\mathbf{x}, \omega))$, which belongs to the orthotropic material symmetry, is taken into account as shown in Table 2 [1]. By setting the coefficient of dispersion of the random elasticity matrix field to $\delta_C = 0.1$, the coefficient of dispersion of the matrix-valued random field $T(\mathbf{x}, \omega)$ is determined using Eq. (69). Accordingly, the fluctuation matrix $T(\mathbf{x}, \omega)$ is modelled as a non-linear transformation of 6 (as $n = 3$, $d = 2$) independent Gaussian random fields, each with a zero mean and unit variance. Here, every standard Gaussian random field is discretized by the proper orthogonal decomposition (also known as the Kosambi-Karhunen-Loève expansion) [24, 21], which is truncated to a fixed 100 terms and further defined by a Gaussian autocorrelation function with a correlation length of 3.5cm in the x and y directions on all four levels of meshes [22, 30].

l	Elements	Nodes	DOF
0	171	206	396
1	684	753	1476
2	2736	2873	5688
3	10944	11217	22320

Table 1: Mesh specifications of 2D meshes

Young's modulus (MPa)	Poisson's ratio	Shear modulus (MPa)
$E_1 = 12000$	$\nu_{21} = 0.371$	$G_{12} = 5610$
$E_2 = 20000$		

Table 2: Orthotropic material parameters

As mentioned in Section 5.3, the objective of the study is to compute the MLMC mean $\hat{\mu}^{\text{ML}}$ and variance \hat{h}_2^{ML} estimates of the total displacement random field $u_{\hat{h}_L}^{(t)}(\mathbf{x}, \omega)$. The procedure for implementation of the scale-invariant MLMC is similar to that of the conventional MLMC method; the only difference is in the usage of normalized error instead of absolute error; see [15] for the algorithm. In this study, we assume that the optimal finest level (here, $L = 3$) is known i.e., the conditions $\hat{\varepsilon}_d^2(\hat{\mu}^{\text{ML}}) < \varepsilon^2/2$ and $\hat{\varepsilon}_d^2(\hat{h}_2^{\text{ML}}) < \varepsilon^2/2$

from Sections (4.1) and (4.2) are met. Therefore, the focus is only on satisfying the condition of normalized sampling errors; in other words, the objective is to ensure that $\hat{\varepsilon}_s(\hat{\mu}^{\text{ML}})$ and $\hat{\varepsilon}_s(\hat{h}_2^{\text{ML}})$ are less than $\varepsilon^2/2$. Furthermore, to avoid the interpolation error, the terms Y_{h_l, N_l} and Z_{h_l, N_l} in Eqs. (34) and (44) are calculated only at finite element nodes that have the same common spatial coordinates between all four levels of meshes. This further means that the MLMC mean and variance estimates of the system response on the finest level L are evaluated only at these common nodes.

6.2 Screening test

An apriori performance analysis of MLMC mean and variance estimators is done by the so-called screening test, in which a fixed number of 50 samples is considered over four levels of meshes. For the MLMC mean estimate, we assume—for simplification—that the estimated normalizing function $\hat{\zeta}_m(u_{h_0, N_0}^{(t)}) = \hat{h}_2^{\text{MC}}(u_{h_0, N_0}^{(t)})$ is spatially constant, i.e., $\hat{\zeta}_m^* = \max(\hat{h}_2^{\text{MC}}(u_{h_0, N_0}^{(t)}))$. With this, by considering a L_∞ norm over the error bounds in Eq. (42) and the second relation in Eq. (41), one obtains:

$$\begin{aligned} \frac{\max |\hat{\mu}^{\text{MC}}(Y_{h_l, N_l})|}{\sqrt{\hat{\zeta}_m^*}} &\leq c_\alpha h_l^\alpha, \\ \frac{\max \left(\hat{h}_2^{\text{MC}}(Y_{h_l, N_l}) \right)}{\hat{\zeta}_m^*} &\leq c_\beta h_l^\beta. \end{aligned} \quad (73)$$

As to the MLMC variance estimate, similar to the assumptions made in the previous equations, one may consider $\hat{\zeta}_v^* = \max(\hat{V}_2^{\text{MC}}(u_{h_0, N_0}^{(t)}))$ as the normalization constant. Thereby, Eq. (55) and the second case in Eq. (53) are rewritten as

$$\begin{aligned} \frac{\max |Z_{h_l, N_l}|}{\sqrt{\hat{\zeta}_v^*}} &\leq c_\alpha h_l^\alpha, \\ \frac{\max \left(\hat{V}_{l, 2}^{\text{MC}} \right)}{\hat{\zeta}_v^*} &\leq c_\beta h_l^\beta. \end{aligned} \quad (74)$$

Following this, Fig. 3 shows an overview of the corresponding results. Note that the normalization constants $\hat{\zeta}_m^*$ and $\hat{\zeta}_v^*$ for the screening test are also set by 50 initial samples. The top left and right plots show the behaviour of the logarithm of ratios defined in Eqs. (73) and (74). The deterministic decay of difference terms $\max |\hat{\mu}^{\text{MC}}(Y_{h_l, 50})|$ and $\max(Z_{h_l, 50})$ can be seen. A stochastic convergence of the quantities $\max(\hat{h}_2^{\text{MC}}(Y_{h_l, 50}))$ and $\max(\hat{V}_{l, 2}^{\text{MC}})$ is also shown in the second plot. Interestingly, one may notice that both the convergences (deterministic and stochastic) pertaining to mean and variance estimates have a similar decay rate. On the other hand, in the top left plot, the quantities $\max(\hat{\mu}^{\text{MC}}(u_{h_l, 50}^{(t)}))$ and $\max(\hat{h}_2^{\text{MC}}(u_{h_l, 50}^{(t)}))$ stay approximately constant at all values of l . Similarly, on the right hand side, the entities $\max(\hat{h}_2^{\text{MC}}(u_{h_l, 50}^{(t)}))$ and $\max(\hat{V}_2^{\text{MC}}(u_{h_l, 50}^{(t)}))$ are also approximately constant for varying values of l —which meets the assumption for consideration of standardising functions $\hat{\zeta}_m$ and $\hat{\zeta}_v$ on coarse mesh $l = 0$ made in Sections (4.1.1) and (4.2.1). Furthermore, the logarithmic computational time of running one sample \mathcal{C}_l on each mesh level l is shown at the bottom. The corresponding values are obtained by recording the timings for the 50 considered screening samples on a 2.3GHz

Intel Core i5 processor with 8GB of RAM and taking the average. As the results show, computing becomes more expensive as the mesh refinement increases.

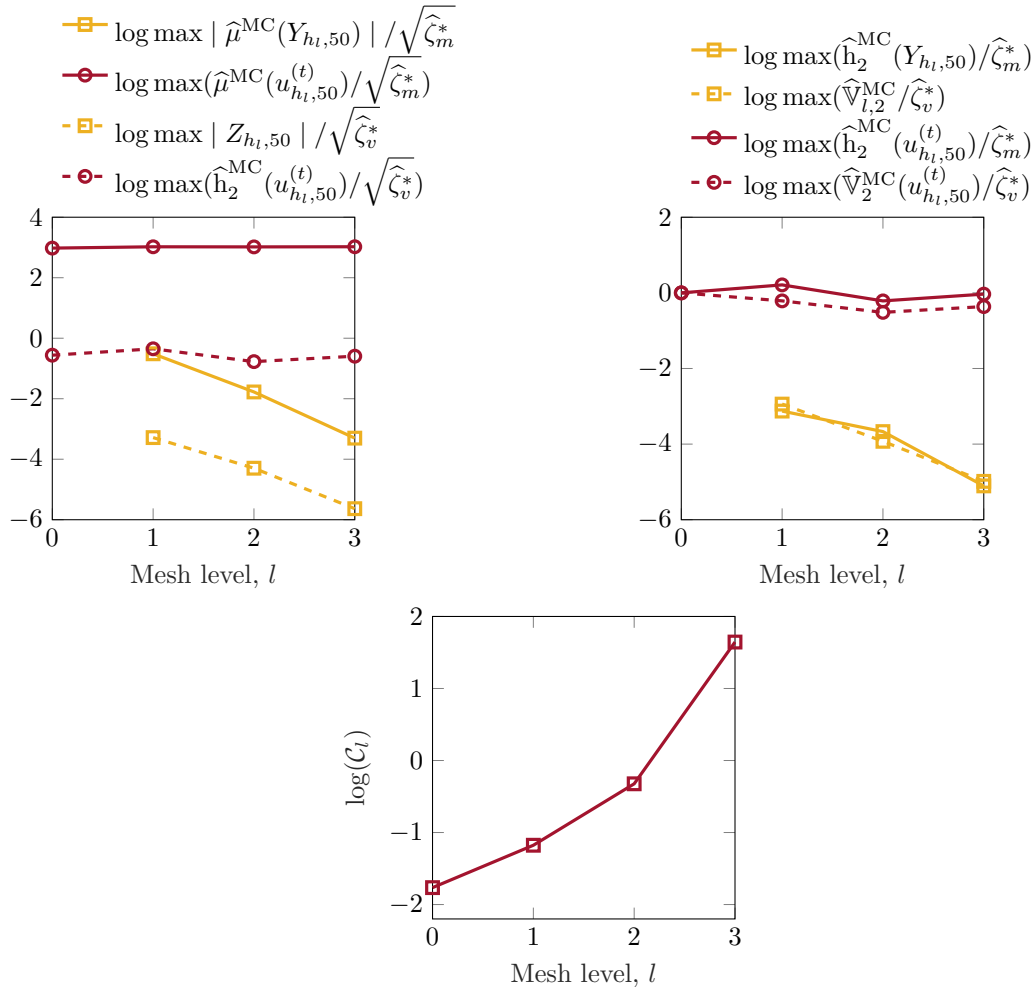


Figure 3: Screening results of MLMC mean estimator

Finally, the decay rates and constants corresponding to Eqs. (73) and (74), as well as the third equation in Eq. (41) are evaluated by determining the slopes and y-intercepts of respective logarithmic quantities in Fig. 3 and are further summarised in Table 3. Clearly, all the constants are positive, and the condition $\alpha \geq \frac{1}{2} \min(\beta, \gamma)$ is satisfied, verifying the assumption made in Propositions. 4.1 and 4.2. One may also notice the approximately equal decay rates α , β and γ for both mean and variance estimators. Also, the constants c_β and c_γ remain the same for both estimates, except c_α , which differs significantly. Moreover, as $\beta < \gamma$, the computational complexity of MLMC estimates follows the third scenario in Eq. (4.1).

Statistic	α	β	γ	c_α	c_β	c_γ
Mean	≈ 2	≈ 1.4	1.6	2.52	≈ 0.1	0.13
Variance				0.13		

Table 3: Convergence results of MLMC mean and variance estimators

6.3 Estimation of total displacement

Figs. 4 and 5 compare the mean and variance estimates of total displacement (TD) of the femoral bone between MC and MLMC. In general, the results are displayed for the

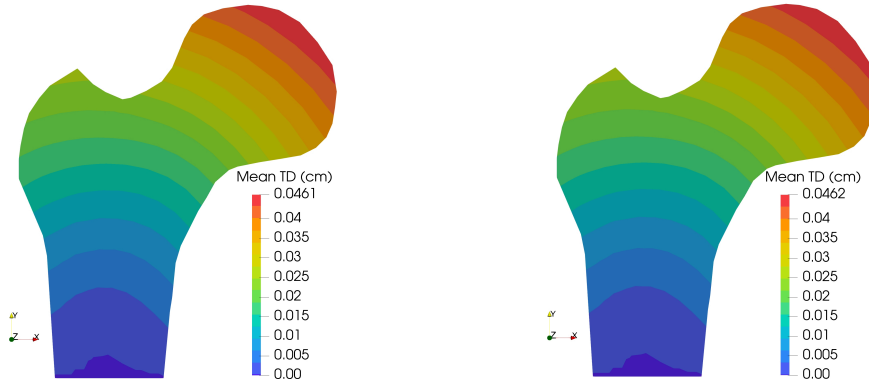


Figure 4: MLMC (on left) and MC (on right) mean estimate of total displacement

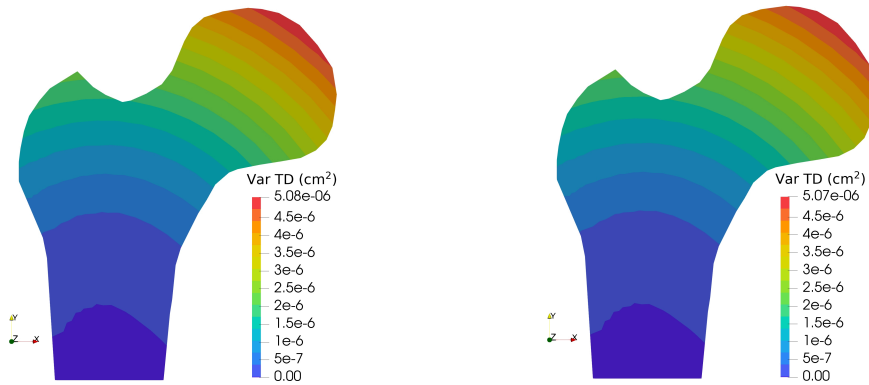


Figure 5: MLMC (on left) and MC (on right) variance estimate of total displacement

normalized mean-squared accuracy of $2e-4$. Note that, as the displacement values are determined on the finest mesh $L = 3$ at the common nodes corresponding to the coarse mesh $l = 0$, the contour plots are mapped directly on this coarse mesh. In Fig. 4, a maximum mean value of approximately 0.046cm can be seen in the region of the pressure load applied. Further, Fig. 5 shows the influence of material uncertainty on the displacement $u_{h_L, \{N_l\}}^{(t)}$ due to the random material model $C(\mathbf{x}, \omega)$. A maximum variance is also witnessed at the top region of the bone. Furthermore, it is clear from both figures that the difference in statistical results between the MLMC and MC methods is small.

6.4 Performance analysis

Fig. 6 shows an overview of the performance of scale-invariant MLMC. The top plot shows the propagation of a maximum number of samples $\max(N_l)$ on each level l for both MLMC mean and variance estimators, corresponding to varying sampling accuracies $\epsilon^2/2$. One may observe that N_l decreases monotonically with increasing l for both estimates. For all of the investigated sampling NMSEs, it is obvious that the variance estimate requires more samples than the mean estimate. The bottom left plot compares the overall cost of MLMC and MC mean and variance estimation to given normalized sampling MSEs. Certainly,

MLMC estimates have a faster convergence rate than the MC approach. Furthermore, the MC cost of mean and variance exhibits non-asymptotic behaviour. Similarly, the cost of MLMC estimates differs, with the variance estimate being relatively more expensive than the mean—as stated in Section 4.2.1. Because scale-invariant error estimates are used in this investigation, it is possible to conclude that the cost of the MLMC mean and variance estimator is asymptotic. The MLMC mean and variance estimates are found to be approximately 6 and 4 times faster than the classical MC mean and variance estimates for all of the NMSEs studied, respectively. In other words, approximate cost savings of 83% and 75% are reported by the mean and variance of MLMC estimates as compared to MC costs. The bottom-right graphic also shows the scale invariance element of the MLMC convergence for an individual statistic in two distinct units (cm and m). Both the MLMC mean (in cm and m) and variance (in cm^2 and m^2) convergence remain unchanged, as can be observed.

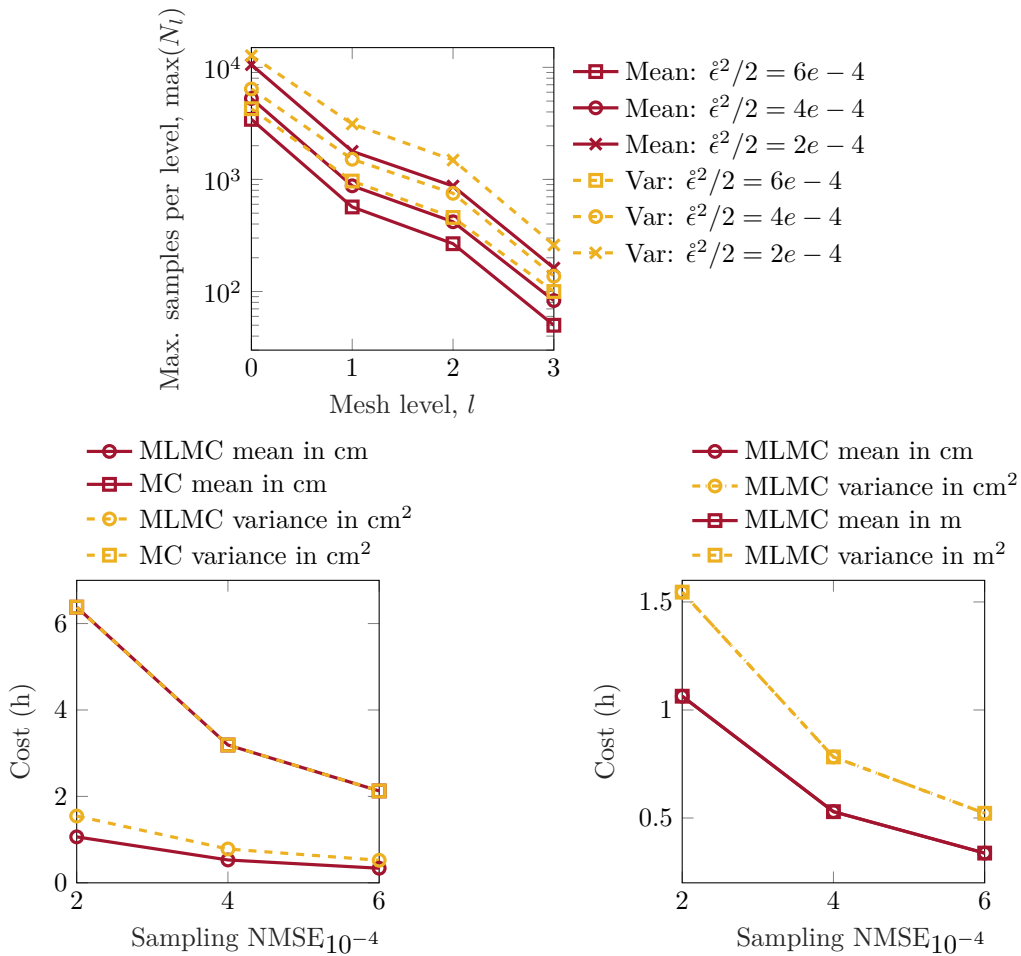


Figure 6: Performance of scale-invariant MLMC mean and variance estimators

Finally, the summary of the given and estimated maximum value of sampling NMSEs of MLMC mean and variance estimators (in cm) is tabulated in Table 4. It can be seen that the achieved maximum NMSEs of mean and variance are within the given limits of $\hat{\epsilon}^2/2$. Furthermore, the maximum absolute sampling MSEs corresponding to the obtained scale-invariant errors, i.e., $\max(\hat{\epsilon}_s(\hat{\mu}^{\text{ML}})) = \hat{\zeta}_m^* \max(\hat{\epsilon}_s(\hat{\mu}^{\text{ML}}))$ and $\max(\hat{\epsilon}_s(\hat{h}_2^{\text{ML}})) = \hat{\zeta}_v^* \max(\hat{\epsilon}_s(\hat{h}_2^{\text{ML}}))$, are also presented in the table. For a given NMSE value, the absolute MSE of variance is much smaller in magnitude as compared to the

mean, which is also on different scales. This emphasises the need for normalized error estimates to ensure easier interpretation of performance between the MLMC estimators.

Given NMSE, $\hat{\epsilon}^2/2$	Estimated NMSE, $\max(\hat{\epsilon}_s(\hat{\mu}^{\text{ML}}))$	Estimated MSE in cm^2
2e-4	1.97e-4	9.459e-10
4e-4	3.99e-4	1.889e-9
6e-4	5.98e-4	2.859e-9

(a) Mean

Given NMSE, $\hat{\epsilon}^2/2$	Estimated NMSE, $\max(\hat{\epsilon}_s(\hat{h}_2^{\text{ML}}))$	Estimated MSE in cm^4
2e-4	1.98e-4	9.387e-15
4e-4	3.89e-4	1.856e-14
6e-4	5.83e-4	2.789e-14

(b) Variance

Table 4: Given and estimated sampling NMSE and corresponding absolute MSE of MLMC estimates

7 Conclusion

We present a novel scale-invariant approach for estimating the MLMC mean and variance. This is accomplished by using t-statistics to normalise the usual absolute error estimates used in classical MLMC approaches. The normalizing factors for mean and variance estimates are formulated to be finite, unbiased, have minimum variance, and remain robust under any linear transformation (such as scaling and addition) of the quantity of interest. We also introduce standardised errors for the MC mean and variance estimators. As a result, the technique lessens ambiguity and facilitates the interpretation of performance analysis between estimations and across various scales.

The scale-invariant MLMC (and MC) method is applied to a linear-elastic material model of a two-dimensional proximal human femur. The analysis considers uncertainties in the material description, which are modelled using a reduced parametric approach that includes heterogeneity and random anisotropy. The method propagates these uncertainties to estimate statistics like the mean and variance of the total displacement.

Through normalized error estimates, we compared the computational efficiencies of MLMC and MC estimators for both mean and variance. MLMC outperforms MC in terms of computational cost for both estimates. However, the variance estimate in MLMC requires a higher number of samples, making it more computationally expensive than the mean estimate. The complete normalization of sampling error reveals non-asymptotic behaviour in the MC cost between mean and variance, while MLMC costs exhibit an asymptotic relationship. Additionally, the difference in accuracy between mean and variance estimates is found to be small between the MLMC and MC methods.

Acknowledgment

The authors gratefully acknowledge the financial support of the German Research Foundation (DFG) within the DFG Priority Program SPP 1748 “Reliable Simulation Techniques in Solid Mechanics”.

References

- [1] R. Ashman, S. Cowin, W. Van Buskirk, and J. Rice. A continuous wave technique for the measurement of the elastic properties of cortical bone. *Journal of Biomechanics*, 17(5):349–361, Jan. 1984.
- [2] A. Barth, C. Schwab, and N. Zollinger. Multi-level Monte Carlo Finite Element method for elliptic PDEs with stochastic coefficients. *Numerische Mathematik*, 119(1):123–161, 2011.
- [3] C. Bierig and A. Chernov. Convergence analysis of multilevel Monte Carlo variance estimators and application for random obstacle problems. *Numerische Mathematik*, 130(4):579–613, Aug. 2015.
- [4] C. Bierig and A. Chernov. Estimation of arbitrary order central statistical moments by the multilevel Monte Carlo method. *Stochastics and Partial Differential Equations Analysis and Computations*, 4(1):3–40, Mar. 2016.
- [5] A. Bóna, I. Bucataru, and M. A. Slawinski. Coordinate-free Characterization of the Symmetry Classes of Elasticity Tensors. *Journal of Elasticity*, 87(2-3):109–132, June 2007.
- [6] E. Cho and M. Cho. Variance of sample variance with replacement. *International Journal of Pure and Applied Mathematics*, 52:43–47, 01 2009.
- [7] K. A. Cliffe, M. B. Giles, R. Scheichl, and A. L. Teckentrup. Multilevel monte carlo methods and applications to elliptic pdes with random coefficients. *Computing and Visualization in Science*, 14(1):3–15, 2011.
- [8] S. C. Cowin. *Continuum Mechanics of Anisotropic Materials*. Springer New York, New York, NY, 2013.
- [9] P. S. Dwyer. Moments of Any Rational Integral Isobaric Sample Moment Function. *The Annals of Mathematical Statistics*, 8(1):21–65, 1937. Publisher: Institute of Mathematical Statistics.
- [10] F. Fahrenndorf, S. Shivanand, B. V. Rosic, M. S. Sarfaraz, T. Wu, L. De Lorenzis, and H. G. Matthies. *Collocation Methods and Beyond in Non-linear Mechanics*, pages 449–504. Springer International Publishing, Cham, 2022.
- [11] R. A. Fisher. 043: Applications of "Student's" Distribution. *Metron*, 5:90–104, 1925.
- [12] G. Fishman. *Monte Carlo: Concepts, Algorithms, and Applications*. Springer Series in Operations Research and Financial Engineering. Springer-Verlag, New York, 1996.

- [13] D. Geraldes and A. Phillips. A comparative study of orthotropic and isotropic bone adaptation in the femur. *International Journal for Numerical Methods in Biomedical Engineering*, 30(9):873–889, 2014.
- [14] M. B. Giles. Multilevel monte carlo path simulation. *Operations Research*, 56(3):607–617, 2008.
- [15] M. B. Giles. Multilevel monte carlo methods. *Acta Numerica*, 24:259–328, 2015.
- [16] C. Graham and D. Talay. *Stochastic Simulation and Monte Carlo Methods: Mathematical Foundations of Stochastic Simulation*. Stochastic Modelling and Applied Probability. Springer-Verlag, Berlin Heidelberg, 2013.
- [17] J. Guilleminot and C. Soize. A stochastic model for elasticity tensors with uncertain material symmetries. *International Journal of Solids and Structures*, 47(22):3121 – 3130, 2010.
- [18] A.-L. Haji-Ali, F. Nobile, E. Von Schwerin, and R. Tempone. Optimization of mesh hierarchies in multilevel Monte Carlo samplers. *Stochastics and Partial Differential Equations Analysis and Computations*, 4(1):76–112, Mar. 2016.
- [19] P. R. Halmos. The Theory of Unbiased Estimation. *The Annals of Mathematical Statistics*, 17(1):34–43, 1946. Publisher: Institute of Mathematical Statistics.
- [20] S. Heinrich. Multilevel Monte Carlo Methods. In *Large-Scale Scientific Computing*, Lecture Notes in Computer Science, pages 58–67. Springer, 2001.
- [21] K. Karhunen. *Über lineare Methoden in der Wahrscheinlichkeitsrechnung*. Suomalaisen Tiedeakatemia toimituksia. Suomalainen Tiedeakatemia, Helsinki, 1947.
- [22] A. Keese. *Numerical Solution of Systems with Stochastic Uncertainties: A General Purpose Framework for Stochastic Finite Elements*. PhD thesis, Technische Universität Braunschweig, 2004.
- [23] T. S. Keller. Predicting the compressive mechanical behavior of bone. *Journal of Biomechanics*, 27(9):1159–1168, 1994.
- [24] D. D. Kosambi. Statistics in function space. *Journal of the Indian Mathematical Society*, 7:76–88, 1943.
- [25] S. Krumscheid, F. Nobile, and M. Pisaroni. Quantifying uncertain system outputs via the multilevel Monte Carlo method — Part I: Central moment estimation. *Journal of Computational Physics*, 414:109466, Aug. 2020.
- [26] O. P. Le Maître and O. M. Knio. *Spectral Methods for Uncertainty Quantification: With Applications to Computational Fluid Dynamics*. Scientific Computation. Springer Netherlands, Dordrecht, 2010.
- [27] N. Metropolis and S. Ulam. The Monte Carlo Method. *Journal of the American Statistical Association*, 44(247):335–341, 1949.
- [28] S. Mishra, C. Schwab, and J. Šukys. Multi-level Monte Carlo finite volume methods for nonlinear systems of conservation laws in multi-dimensions. *Journal of Computational Physics*, 231(8):3365–3388, Apr. 2012.

- [29] C. Rose and M. Smith. *Mathematical statistics with Mathematica.*, volume 481. New York, NY: Springer, 2002.
- [30] B. Rosić. *Variational formulations and functional approximation algorithms in stochastic plasticity of materials*. PhD thesis, Technische Universität Braunschweig, 2012.
- [31] V. Sansalone, D. Gagliardi, C. Desceliers, V. Bousson, J. Laredo, F. Peyrin, G. Haiat, and S. Naili. Stochastic multiscale modelling of cortical bone elasticity based on high-resolution imaging. *Biomechanics and Modeling in Mechanobiology*, 15(1):111–131, Feb 2016.
- [32] C. Soize. Non-gaussian positive-definite matrix-valued random fields for elliptic stochastic partial differential operators. *Computer methods in applied mechanics and engineering*, 195(1):26–64, 2006.
- [33] C. Soize. Tensor-valued random fields for meso-scale stochastic model of anisotropic elastic microstructure and probabilistic analysis of representative volume element size. *Probabilistic Engineering Mechanics*, 23(2):307 – 323, 2008.
- [34] Student. The Probable Error of a Mean. *Biometrika*, 6(1):1–25, 1908. Publisher: [Oxford University Press, Biometrika Trust].
- [35] T. Sullivan. *Introduction to Uncertainty Quantification*, volume 63 of *Texts in Applied Mathematics*. Springer International Publishing, Cham, 2015.
- [36] A. L. Teckentrup, R. Scheichl, M. B. Giles, and E. Ullmann. Further analysis of multilevel Monte Carlo methods for elliptic PDEs with random coefficients. *Numerische Mathematik*, 125(3):569–600, Nov. 2013.
- [37] D. S. Tracy and B. C. Gupta. Generalized h -Statistics and Other Symmetric Functions. *The Annals of Statistics*, 2(4):837–844, 1974. Publisher: Institute of Mathematical Statistics.
- [38] D. Xiu. *Numerical methods for stochastic computations: a spectral method approach*. Princeton University Press, Princeton, N.J, 2010. OCLC: ocn466341417.
- [39] Z. Yosibash, R. Padan, L. Joskowicz, and C. Milgrom. A CT-Based High-Order Finite Element Analysis of the Human Proximal Femur Compared to In-vitro Experiments. *Journal of Biomechanical Engineering*, 129(3):297–309, June 2007.